

Probing Vortex Dynamics in 2D Superconductors with Scanning Quantum Microscope

Sreehari Jayaram^{1†}, Malik Lenger^{1†}, Dong Zhao^{2,3,4}, Lucas Pupim⁵, Takashi Taniguchi⁶, Kenji Watanabe⁷, Ruoming Peng^{1*}, Marc Scheffler⁸, Rainer Stöhr¹, Mathias S. Scheurer⁵, Jurgen Smet², Jörg Wrachtrup^{1,2}

¹3rd Institute of Physics, University of Stuttgart, Allmandring 13, Stuttgart, 70569, Baden-Württemberg, Germany.

²Max-Planck-Institute for Solid State Research, Heisenbergstrasse 1, Stuttgart, 70569, Baden-Württemberg, Germany.

³Beijing National Laboratory for Condensed Matter Physics, Institute of Physics, Chinese Academy of Sciences, , Beijing, 100190, China.

⁴School of Physical Sciences, University of Chinese Academy of Sciences, , Beijing, 100049, China.

⁵Institute for Theoretical Physics III, University of Stuttgart, Pfaffenwaldring 57, Stuttgart, 70569, Baden-Württemberg, Germany.

⁶Research Center for Materials Nanoarchitectonics, National Institute for Materials Science, 1-1, Namiki, 305-0044, Tsukuba, Japan.

⁷Research Center for Electronic and Optical Materials, National Institute for Materials Science, 1-1, Namiki, 305-0044, Tsukuba, Japan.

⁸1st Institute of Physics, University of Stuttgart, Pfaffenwaldring 57, Stuttgart, 70569, Baden-Württemberg, Germany.

*Corresponding author(s). E-mail(s): pruoming@gmail.com;

†These authors contributed equally to this work.

Abstract

The visualization of the magnetic responses of a two-dimensional (2D) superconducting material on the nanoscale is a powerful approach to unravel the underlying supercurrent behavior and to investigate critical phenomena in reduced dimensions. In this study, scanning quantum microscopy is utilized to explore the local magnetic response of the 2D superconductor 2H-NbSe₂. Our technique enables both static and dynamic sensing of superconducting vortices with high sensitivity and a spatial resolution down to 30 nm, unveiling unexpected phenomena linked to the intrinsic 2D nature of the superconductor, which are challenging to detect with more conventional local probes. Vortices do not arrange in a hexagonal lattice, but form a distorted vortex glass with expanding vortex size. A vortex can exhibit strong local dynamics due to thermal excitation. As the critical temperature is approached, a clear melting of the vortex glass is identified, leading to distinct configurations under different cooling conditions. Vortex fluctuations can also be probed through spin Hahn-echo measurements, which reveal the spin decoherence even well below the critical temperature — and, intriguingly, enhanced decoherence at lower temperatures. Spatiotemporal microscopy of the magnetic dynamics associated with vortex excitations and fluctuations provides direct evidence of 2D superconducting phenomena at the nanoscale.

Keywords: NV center, Scanning probe microscopy, 2D Superconductor, NbSe₂, Type-II superconductor, superconducting vortex

1 Introduction

Two-dimensional (2D) superconductors offer a versatile platform for exploring novel interactions and quantum phenomena. Their reduced dimensionality and consequently enhanced fluctuations manifest not only in the superfluid condensate but also in the excitations, such as vortices. In bulk type-II superconductors, vortices induced by an externally applied magnetic field form well-ordered hexagonal lattices referred to as Abrikosov vortex crystals [1]. In 2D superconductors, however, the behavior of vortices is distinct. It is governed by thickness-related strong confinement, an enhanced susceptibility to disorder, as well as quantum correlation [2]. As a result, the vortices in a 2D superconductor are predicted to expand. They evolve into the so-called Pearl vortices [3], and arrange into a glassy state without translational invariance. Concurrently, delocalization of vortices can become pervasive [4–6], especially near the critical temperature (T_c), where the vortex lattice is predicted to melt into a liquid phase [7–9]. The presence of defects and dislocations can also influence the vortex configuration, and a variety of vortex phases may form, such as a pinned vortex glass, a stripe vortex liquid, and ultimately, an isotropic vortex liquid [10]. In disordered systems, fluctuations can drive both thermodynamic and quantum phase transitions. Examples unique to 2D systems include the Berezinskii-Kosterlitz-Thouless (BKT) transition [11–13] and the metal-to-insulator transition [14]. Beyond this vortex physics, 2D superconductors exhibit many other unconventional phenomena, including critical fields far beyond the Pauli limit [15], a layer-dependent T_c [16], unusual pairing symmetries [17, 18], and unconventional finite momentum pairing as in the so-termed orbital Fulde-Ferrell-Larkin-Ovchinnikov state [19, 20].

So far, electrical transport [16], terahertz (THz) spectroscopy [?], and magnetic susceptibility measurements [14, 15, 22] have been conducted to probe the static and dynamic responses of crystalline 2D superconductors. These experimental techniques have revealed macroscopic signatures of superconductivity with complex pairing symmetries and vortex arrangements. To investigate nanoscale superconducting phenomena, scanning tunneling microscopy (STM) has been widely employed to map the local density of states [23? , 24]. However, due to the tunneling nature of such probes, the system requires an ultra-clean conducting surface. Surface residues left behind during thin flake exfoliation or sample fabrication can seriously hamper such STM studies. The frequently used hexagonal boron nitride (hBN) cladding layer to protect air-sensitive 2D flakes is also problematic [25–27]. When approaching the 2D limit, thermal fluctuations play a crucial role for the electron behavior [4, 28, 29]. They influence collective phenomena such as the dynamics of vortices. STM, as well as conventional nanoscale probes [30], such as magnetic force microscopy (MFM), and nano superconducting quantum interference devices (nano-SQUIDs), do not simultaneously offer the required spatial and temporal resolution to capture this emergent magnetic dynamics.

To overcome these limitations and visualize local magnetic excitations with the spatiotemporal resolution necessary for the 2D superconductors, scanning quantum microscope (SQM) based on nanoscale magnetometry with single nitrogen vacancy (NV) centers in diamond, has been developed [31, 32]. Supercurrent flows in cuprate superconductors with a critical temperature (T_c) of 89 K were visualized. Single vortices and the effective penetration depth were characterized in a quantitative manner [33, 34]. The quantum sensing community has also extended the toolbox for SQM with numerous pulse sequences to extend its dynamic range [35, 36]. Among others, screening effects associated with superconductivity were investigated, demonstrating the ability of SQM to detect surface charge noise in the diamond substrate [37]. So far, SQM has primarily been applied to address the static response of high- T_c superconductors. Extending its application to two-dimensional superconductors holds great promise, since the local dynamic response of 2D superconductors should be particularly rich, but remains largely unexplored, which is the purpose of this work.

We visualize the local magnetic response of few-layer NbSe₂ with SQM. In contrast to the hexagonal Abrikosov vortex lattice observed in bulk superconductors, we detect a distorted vortex glass. By varying the cooling rate, we capture the stochastic process of vortex glass condensation. Furthermore, dynamic spin decoherence measurements reveal an unusual temperature dependence of the fluctuations with enhanced magnetic noise persisting to temperatures well below the critical temperature. By combining high temporal and spatial resolution within our SQM technique, we have succeeded in recording the in-plane magnetic dynamics within the disordered vortex glass

that forms in a 2D superconductor due to enhanced thermal fluctuations and incomplete screening within the superconductor.

2 Local vortex excitation in the 2D superconductor

Our measurements were performed on samples out of thin layers of the 2D superconductor 2H-NbSe₂ using a 1.8 K cryogenic atomic force microscope (AFM), where the cantilever of the AFM probe is fabricated from a diamond slab with a shallow implanted NV positioned at the apex of the diamond pillar, as illustrated in Fig. 1a. As the NV center approaches the NbSe₂ sample (S1), the spin of a single NV can detect the local magnetic responses of the NbSe₂ irrespective of the top hBN cladding (see supplementary information (SI) section 1 for details). The NbSe₂ flake consists of two regions with different thicknesses: 5.1 nm (7 layers) and 12.6 nm. An optical image and AFM scan are shown in Fig. S1 in the SI. In the thinner NbSe₂, three distinct phases — vortex glass (VG), vortex liquid (VL), and metallic (M) state — are illustrated, as shown in Fig. 1b. These phases have been previously characterized through transport measurements, revealing the transitions between superconducting and dissipative states [38]. The melting temperature is denoted as T_M , while H_{c1} and H_{c2} represent the lower and upper critical fields, respectively, for a type-II superconductor. Fig. 1c presents a scan recorded for the vortex glass state with a diamagnetic response along the flake edge at a temperature of 2 K, indicative of the Meissner effect. Near 10 K ($> T_c$), any magnetic response has vanished (Fig. S4 in SI), confirming that the observed magnetic behavior at 2 K originates from the superconducting state. Since the flake’s thickness is significantly smaller than the penetration depth λ of bulk NbSe₂ ($\lambda \sim 125$ nm) [39, 40], the external magnetic field is only partially screened by the 2D superconductors. The effective field screening is approximately $-100 \mu\text{T}$.

Here, we also observe a positive magnetic signal, attributed to superconducting vortices that persist throughout almost the entire superconducting phase. Notably, vortices emerge under external fields as low as a few mT, significantly below the reported first critical field (B_{c1}) for bulk NbSe₂. Due to the few-layer thickness of the sample, the magnetic field readily penetrates the material, locally suppressing superconductivity and forming vortices at a much lower external field. The vertical confinement in the very thin NbSe₂ layer causes an expansion of the vortex, following the Pearl model [3]. From a high-resolution scan of a single vortex in Fig. 1d, the size of the vortex is expanding compared to the vortex in the bulk, matching the expected scaling behavior for Pearl vortices in thin-layer superconductors [41]. It is proportional to $2\lambda^2/d$, where d is the flake thickness.

Sample characterization with Atomic Force Microscopy (AFM) (Fig. S1 in SI) reveals significant residue on the flake surface after sample fabrication. Such a dirty top surface poses technical challenges for other local probes such as scanning tunneling microscopy (STM) [42, 43]. The SQM technique put forward here is obviously more robust. It enables high-resolution and non-invasive mapping of the superconducting vortices. The surface residues may introduce small deviations in the measured magnetic field map, but these can be corrected for a posteriori by correlating field maps with AFM topography data.

3 Arrangement of the vortices in 2D superconductor

In the thin NbSe₂ sample (S1), substrate roughness, disorder and finite-size effects play an important role in the superconducting response. Due to these local effects, vortices can become distorted and elongated, so their shape deviates from the regular vortex shape typically observed in a pristine superconductor. Because of the multiband nature of superconductivity in NbSe₂ [44, 45], multiple-flux-quanta vortices [46] may appear. Fig. 2a shows an example data set where no clear hexagonal vortex arrangement can be discerned. The autocorrelation pattern in Fig. 2b reveals a highly distorted vortex arrangement with elongated and irregular features that blur the vortices of the correlation peaks. An underlying hexagonal pattern can barely be recognized. As seen in Fig. S5 of the SI, the auto-correlation pattern varies in a distinct pattern as the scanning area is moved away from the edge to the center of the sample. Near the edge, the vortex configuration is strongly constrained by the sample boundary, and features in the autocorrelation signal align with the orientation of the edge. In contrast, toward the center, the arrangement is increasingly governed by

intrinsic vortex interactions. Hexagonal ordering appears more clearly, but it remains significantly influenced by local disorder.

Thin samples also show features that appear like elongated vortices, as indicated in Fig. 2a, for temperature well below T_c . We attribute these line-shaped magnetic field structures to basically circular vortices that rapidly fluctuate between distinct positions in space, i.e. they are somewhat delocalized, effectively causing the elongated shapes in the SQM images. This vortex motion is likely mediated by the underlying disorder and the enhanced thermal fluctuations in a 2D superconductor [47]. For the sake of comparison, we performed similar measurements on a larger and thicker NbSe₂ sample (>10 nm, S2) encapsulated on both sides with hBN to ensure flat and pristine samples (Fig. S2 in SI). In this case, vortices arrange in a more orderly fashion and a hexagonal vortex lattice is observed in most of the sample area (Fig. 2c). Subsequent autocorrelation analysis of different regions (Fig. 2d) reveal a natural Abrikosov vortex arrangement, although it remains distorted due to the competition with geometric confinement and spatial disorder. We note that the lack of knowledge about the specific and non-hexagonal vortex arrangement in thinner samples may be important for the interpretation of, for instance, transport experiments. This is frequently overlooked, yet may be important for a proper deduction of the symmetry of the superconducting ground state from such experimental data.

4 Melting transition of the vortex lattice

Previous transport studies on thin NbSe₂ samples have also provided indirect evidence that the melting of the vortex glass takes place more easily than in bulk systems. The strong thermal fluctuations can depin vortices and drive the melting transition [38]. The observation of non-zero resistivity across a broader temperature window, but still below T_c , indeed suggested that vortices detach from their pinning site and make a transition into the vortex liquid phase. Such melting can be further promoted by the presence of dislocations [10, 48]. Since the vortex melting process is influenced by local disorders present in the flake, one may argue that the relaxation of the vortex liquid likely evolves differently as the cooling speed is varied. SQM is well suited to address such cooling rate-dependent physics as it can detect both the vortex lattice itself as well as the melting of the vortex lattice.

Therefore, we have performed such a study with varied cooling cycles. For each cooling sequence, the sample is “initialized” by raising the temperature to 6.3 K. This is still below $T_c=6.8$ K, but at this temperature only a weak magnetic field response remains, and isolated vortices are no longer visible in a large-area scan (See Fig. S5 in SI). The zoom-in scan reveals weak magnetic signals without distinct vortex features (See Fig. S6 in SI). Subsequently, the sample is cooled to base temperature at the selected rate. This procedure is repeated for different cooling rates from 1 minute up to 10 hours until the base temperature of 2 K. The SQM measurements for the lowest and highest cooling rates are shown in Fig. 3a and 3c. Although both measurements focus on the same location of the few-layer sample, the supercurrent distribution for fast and for slow cooling speed shows a different Meissner field response as well as vortex intensity.

The difference is further enhanced in the autocorrelation graph, shown in Fig. 3b and 3d. We observe an enhancement in absolute autocorrelation intensities under slow cooling conditions. Distinct variations in autocorrelation patterns suggest a redistribution of supercurrent densities driven by different cooling protocols. For a rapid cool down from the melted state, one may anticipate that vortices are not localized or pinned as strongly as upon slow cooling. The abrupt temperature drop causes immediate pinning at surrounding disorder sites, and these pinned vortices remain more susceptible to thermal fluctuations, resulting in a more ‘volatile’ vortex configuration with vortex delocalized on a small length scale and an overall weaker magnetic response. In contrast, slow cooling from the melted state should allow thermal fluctuations to compete with disorder pinning, so that a more stable vortex lattice is gradually formed. This unique phenomenon in 2D superconductors can be visualized in our thin layer of NbSe₂ by mapping the local magnetic field with high spatial resolution for the vortex melting state as well as the cooling-rate-dependent supercurrent distribution.

5 Dynamics in the vortex state

Beyond static measurements, the NV spin offers dynamic magnetic field sensing capabilities across a broad frequency range [36]. By employing tailored pulse sequences, we can isolate and target specific noise sources affecting the spin, thereby improving the spectral selectivity of dynamic measurements. For example, the spin T_1 time is sensitive to magnetic noise in the GHz frequency range, while the spin Hahn echo T_2 enables selective detection within the MHz range. The pulse capability makes NV-based techniques essential tools for investigating fluctuation phenomena in 2D superconductors. Notably, significant fluctuations are expected to arise both from the thermal excitation of quasi-particles, even at temperatures below T_c [49, 50], and from fluctuations of the superconducting order parameter [51]. As illustrated in Fig. 4a, the supercurrent fluctuation can induce strong transverse magnetic noise, leading to the dephasing of the NV electron spin.

We probe the underlying magnetic noise arising from NbSe₂ by conducting Hahn echo measurements of the NV electron spin in proximity to the sample. Compared to the out-of-contact condition, there is a noticeable reduction in the T_2 time, as can be seen in Fig. 4b. The Hahn echo T_2 measurements indicate the presence of magnetic noise in the vortex glass state with frequencies spanning from tens of kHz to MHz. We also characterize spin decoherence as a function of the lift-off distance from the sample surface of the tip and find a clear trend, as shown in Fig. 4c: spin coherence time decreases as the probe approaches the superconducting sample. From this behavior, we deduce a characteristic length scale of several hundred nanometers of the noise source (i.e. vortex movement) underneath the tip. It also represents direct evidence that the vortex in a 2D superconductor itself acts as the primary source of decoherence. Since no significant decoherence is observed in other thick superconducting samples, such as the 300 nm cuprate samples shown in Fig. S9, we attribute the noise to the intrinsic two-dimensional nature of the thin NbSe₂ layer. To quantify the magnetic noise, the spin decoherence rate, $1/T_2$, was measured at different temperatures and compared with the spin decoherence rate in the out-of-contact condition. This data set shows that the NbSe₂-induced change in the decoherence rate is larger at lower temperatures and much less pronounced when the temperature approaches or is above T_c .

Since fluctuations of the superconducting order parameter are expected to be largest in the vicinity of T_c [51] and contributions from quasi-particle excitations should decay with temperature [49, 50], this observation seems surprising at first sight. However, it is important to note that $1/T_2$, unlike $1/T_1$, is primarily sensitive to frequencies in the MHz range such that the aforementioned contributions may not play a dominant role. Instead, the thermally activated motion of the vortex glass is likely the primary factor limiting T_2 . While vortex motion itself decreases as temperature is lowered, it is the resulting magnetic field fluctuations at the NV site that drive decoherence. The magnetic field distribution around vortices in thin superconductors depends critically on the ratio of penetration depth λ and thickness d . Since λ diverges at T_c and decreases as temperature is reduced, the local magnetic field at the NV center becomes increasingly sensitive to vortex position, leading to enhanced decoherence. This mechanism explains the increase in the decoherence rate with decreasing temperature shown in Fig. 4d.

To understand this more explicitly, we solved a Langevin equation, as a simple model for vortex motion at finite temperature, and then computed the resulting magnetic field fluctuations at the NV center to obtain a temperature-dependent decoherence rate (see SI section 3 for details). Even this simple model, requiring minimal assumptions, reproduces the temperature-dependent behavior of $1/T_2$ observed in Fig. 4d (model shown as a solid line). Within the vortex core, the supercurrent flow is suppressed, resulting in minimal magnetic field fluctuations affecting the NV spin.

6 Conclusion

In conclusion, we have successfully achieved nanoscale spatiotemporal imaging of vortices in few-layer 2D superconductors. This has enabled the first direct visualization of multiple 2D superconducting phenomena that were previously only accessible with indirect measurements. The confined geometry of a two-dimensional superconductor leads to a distorted vortex lattice and an expansion of the vortex core size. In non-uniform NbSe₂, deformed and dynamic vortex lines emerge, and vortex melting can be directly visualized. The resulting vortex configuration is found to be highly sensitive to the cooling rate, indicating that it is governed by the interplay between

thermal fluctuations and random pinning sites. Both the spatial arrangement and dynamic behavior of vortices at low magnetic fields have significant implications for the collective macroscopic response of the system, as probed by transport measurements, nuclear magnetic resonance (NMR), and terahertz (THz) spectroscopy. Furthermore, our measurement technique reveals unexpected magnetic noise arising from vortex fluctuations in the vortex glass phase of the 2D superconductor. This observation provides direct evidence that vortex dynamics persists even far below the critical temperature, highlighting the nontrivial role of low-temperature fluctuations and the inherently glassy nature of the vortex state in reduced dimensionality. It also highlights SQM as a powerful probe of low-energy fluctuations and complex electronic states with a large dynamic range, offering nanoscale access to dynamic phenomena in unconventional superconductors [52–55].

References

- [1] Hess, H., Robinson, R., Dynes, R., Valles Jr, J. & Waszczak, J. Scanning-tunneling-microscope observation of the abrikosov flux lattice and the density of states near and inside a fluxoid. *Physical review letters* **62**, 214 (1989).
- [2] Clem, J. R. Two-dimensional vortices in a stack of thin superconducting films: A model for high-temperature superconducting multilayers. *Physical Review B* **43**, 7837 (1991).
- [3] Pearl, J. Current distribution in superconducting films carrying quantized fluxoids. *Applied Physics Letters* **5**, 65–66 (1964).
- [4] Fisher, D. S., Fisher, M. P. & Huse, D. A. Thermal fluctuations, quenched disorder, phase transitions, and transport in type-ii superconductors. *Physical Review B* **43**, 130 (1991).
- [5] Chiang, T.-C. Superconductivity in thin films. *Science* **306**, 1900–1901 (2004).
- [6] Saito, Y., Nojima, T. & Iwasa, Y. Highly crystalline 2d superconductors. *Nature Reviews Materials* **2**, 1–18 (2016).
- [7] Huberman, B. & Doniach, S. Melting of two-dimensional vortex lattices. *Physical Review Letters* **43**, 950 (1979).
- [8] Brandt, E. Thermal fluctuation and melting of the vortex lattice in oxide superconductors. *Physical review letters* **63**, 1106 (1989).
- [9] Koshelev, A. & Vinokur, V. Dynamic melting of the vortex lattice. *Physical review letters* **73**, 3580 (1994).
- [10] Guillaumón, I. *et al.* Direct observation of melting in a two-dimensional superconducting vortex lattice. *Nature Physics* **5**, 651–655 (2009).
- [11] Berezinskii, V. Destruction of long-range order in one-dimensional and two-dimensional systems having a continuous symmetry group i. classical systems. *Sov. Phys. JETP* **32**, 493–500 (1971).
- [12] Kosterlitz, J. M. & Thouless, D. Long range order and metastability in two dimensional solids and superfluids.(application of dislocation theory). *Journal of Physics C: Solid State Physics* **5**, L124 (1972).
- [13] Ryzhov, V. N., Tareyeva, E., Fomin, Y. D. & Tsiok, E. N. Berezinskii–kosterlitz–thouless transition and two-dimensional melting. *Physics-Uspekhi* **60**, 857 (2017).
- [14] Gömöry, F. Characterization of high-temperature superconductors by ac susceptibility measurements. *Superconductor Science and Technology* **10**, 523 (1997).
- [15] Sohn, E. *et al.* An unusual continuous paramagnetic-limited superconducting phase transition in 2d nbse 2. *Nature materials* **17**, 504–508 (2018).

- [16] Xi, X. *et al.* Ising pairing in superconducting NbSe₂ atomic layers. *Nature Physics* **12**, 139–143 (2016).
- [17] Hamill, A. *et al.* Two-fold symmetric superconductivity in few-layer NbSe₂. *Nature physics* **17**, 949–954 (2021).
- [18] Cho, C.-w. *et al.* Nodal and nematic superconducting phases in NbSe₂ monolayers from competing superconducting channels. *Physical Review Letters* **129**, 087002 (2022).
- [19] Zhao, D. *et al.* Evidence of finite-momentum pairing in a centrosymmetric bilayer. *Nature Physics* **19**, 1599–1604 (2023).
- [20] Wan, P. *et al.* Orbital fulde–ferrell–larkin–ovchinnikov state in an ising superconductor. *Nature* **619**, 46–51 (2023).
- [21] Beck, M. *et al.* Energy-gap dynamics of superconducting NbN thin films studied by time-resolved terahertz spectroscopy. *Physical Review Letters* **107**, 177007 (2011).
- [22] Zhu, X. *et al.* Signature of coexistence of superconductivity and ferromagnetism in two-dimensional NbSe₂ triggered by surface molecular adsorption. *Nature communications* **7**, 11210 (2016).
- [23] Hess, H., Robinson, R. & Waszczak, J. Vortex-core structure observed with a scanning tunneling microscope. *Physical review letters* **64**, 2711 (1990).
- [24] Fischer, Ø., Kugler, M., Maggio-Aprile, I., Berthod, C. & Renner, C. Scanning tunneling spectroscopy of high-temperature superconductors. *Reviews of Modern Physics* **79**, 353–419 (2007).
- [25] Watanabe, K., Taniguchi, T. & Kanda, H. Direct-bandgap properties and evidence for ultraviolet lasing of hexagonal boron nitride single crystal. *Nature materials* **3**, 404–409 (2004).
- [26] Dean, C. R. *et al.* Boron nitride substrates for high-quality graphene electronics. *Nature nanotechnology* **5**, 722–726 (2010).
- [27] Roy, S. *et al.* Structure, properties and applications of two-dimensional hexagonal boron nitride. *Advanced Materials* **33**, 2101589 (2021).
- [28] Doniach, S. Quantum fluctuations in two-dimensional superconductors. *Physical Review B* **24**, 5063 (1981).
- [29] Glazman, L. & Koshelev, A. Thermal fluctuations and phase transitions in the vortex state of a layered superconductor. *Physical Review B* **43**, 2835 (1991).
- [30] de Lozanne, A. Scanning probe microscopy of high-temperature superconductors. *Superconductor Science and Technology* **12**, R43 (1999).
- [31] Balasubramanian, G. *et al.* Nanoscale imaging magnetometry with diamond spins under ambient conditions. *Nature* **455**, 648–651 (2008).
- [32] Maletinsky, P. *et al.* A robust scanning diamond sensor for nanoscale imaging with single nitrogen-vacancy centres. *Nature nanotechnology* **7**, 320–324 (2012).
- [33] Thiel, L. *et al.* Quantitative nanoscale vortex imaging using a cryogenic quantum magnetometer. *Nature nanotechnology* **11**, 677–681 (2016).
- [34] Pelliccione, M. *et al.* Scanned probe imaging of nanoscale magnetism at cryogenic temperatures with a single-spin quantum sensor. *Nature nanotechnology* **11**, 700–705 (2016).

- [35] Degen, C. L., Reinhard, F. & Cappellaro, P. Quantum sensing. *Reviews of modern physics* **89**, 035002 (2017).
- [36] Levine, E. V. *et al.* Principles and techniques of the quantum diamond microscope. *Nanophotonics* **8**, 1945–1973 (2019).
- [37] Monge, R. *et al.* Spin dynamics of a solid-state qubit in proximity to a superconductor. *Nano letters* **23**, 422–428 (2023).
- [38] Zhang, E. *et al.* Nonreciprocal superconducting nbse2 antenna. *Nature communications* **11**, 5634 (2020).
- [39] Callaghan, F., Laulajainen, M., Kaiser, C. & Sonier, J. Field dependence of the vortex core size in a multiband superconductor. *Physical review letters* **95**, 197001 (2005).
- [40] Fletcher, J. *et al.* Penetration depth study of superconducting gap structure of 2 h-nbse 2. *Physical review letters* **98**, 057003 (2007).
- [41] Fridman, N. *et al.* Anomalous thickness dependence of the vortex pearl length in few-layer nbse2. *Nature Communications* **16**, 2696 (2025).
- [42] Zomer, P., Guimarães, M., Brant, J., Tombros, N. & Van Wees, B. Fast pick up technique for high quality heterostructures of bilayer graphene and hexagonal boron nitride. *Applied Physics Letters* **105** (2014).
- [43] Pizzocchero, F. *et al.* The hot pick-up technique for batch assembly of van der waals heterostructures. *Nature communications* **7**, 11894 (2016).
- [44] Zehetmayer, M. & Weber, H. Experimental evidence for a two-band superconducting state of nbse 2 single crystals. *Physical Review B—Condensed Matter and Materials Physics* **82**, 014524 (2010).
- [45] Noat, Y. *et al.* Quasiparticle spectra of 2 h-nbse 2: Two-band superconductivity and the role of tunneling selectivity. *Physical Review B* **92**, 134510 (2015).
- [46] Gozliniski, T. *et al.* Band-resolved caroli–de gennes–matricon states of multiple-flux-quanta vortices in a multiband superconductor. *Science Advances* **9**, eadh9163 (2023).
- [47] Schmid, A. & Hauger, W. On the theory of vortex motion in an inhomogeneous superconducting film. *Journal of Low Temperature Physics* **11**, 667–685 (1973).
- [48] Soibel, A. *et al.* Imaging the vortex-lattice melting process in the presence of disorder. *Nature* **406**, 282–287 (2000).
- [49] Chatterjee, S. *et al.* Single-spin qubit magnetic spectroscopy of two-dimensional superconductivity. *Physical Review Research* **4**, L012001 (2022).
- [50] Dolgirev, P. E. *et al.* Characterizing two-dimensional superconductivity via nanoscale noise magnetometry with single-spin qubits. *Physical Review B* **105**, 024507 (2022).
- [51] Curtis, J. B. *et al.* Probing the Berezinskii-Kosterlitz-Thouless vortex unbinding transition in two-dimensional superconductors using local noise magnetometry. *Phys. Rev. B* **110**, 144518 (2024).
- [52] Ge, J. *et al.* Charge-4 e and charge-6 e flux quantization and higher charge superconductivity in kagome superconductor ring devices. *Physical Review X* **14**, 021025 (2024).
- [53] Tanaka, Y. Soliton in two-band superconductor. *Physical review letters* **88**, 017002 (2001).

- [54] Kirtley, J. *et al.* Direct imaging of integer and half-integer josephson vortices in high- T_c grain boundaries. *Physical review letters* **76**, 1336 (1996).
- [55] Iguchi, Y. *et al.* Superconducting vortices carrying a temperature-dependent fraction of the flux quantum. *Science* **380**, 1244–1247 (2023).

Acknowledgements

S.J., M.L., R.P., R.S. J.W. acknowledge funding support by the DFG via FOR 2724 and the RTG GRK 2642, the EU via the AMADEUS project, BMBF via project QSOLID 13N16159 and QMAT 03ZU2110HA, and the Zeiss Foundation through the QPhoton. J.H.S. acknowledges funding support from the DFG Priority Program SPP 2244. L.P. and M.S.S. acknowledge funding by the European Union (ERC-2021-STG, Project 101040651—SuperCorr). Views and opinions expressed are however those of the authors only and do not necessarily reflect those of the European Union or the European Research Council Executive Agency. Neither the European Union nor the granting authority can be held responsible for them.

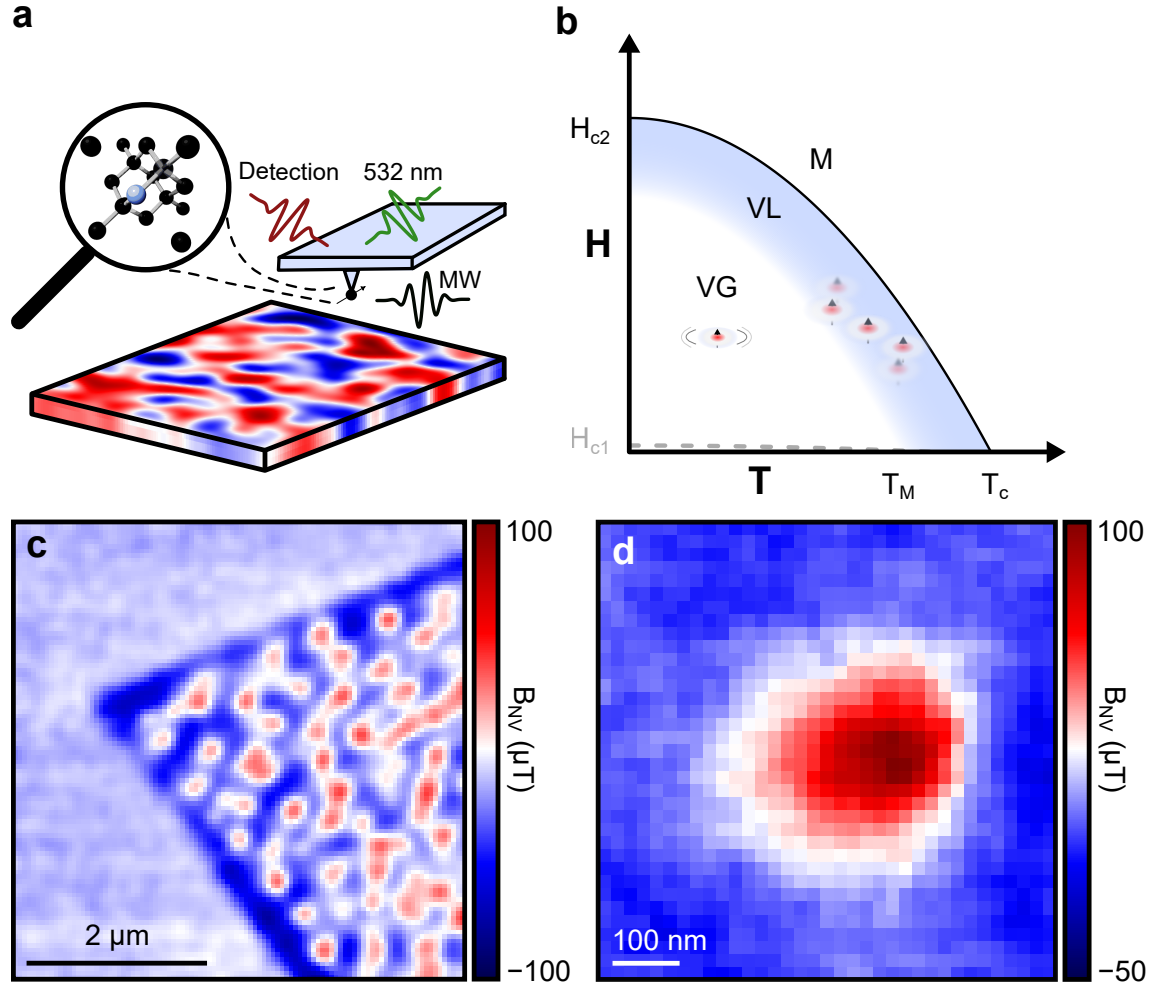


Fig. 1 Scanning quantum microscopy of the vortex state in 2D superconductors. (a) Schematic of the scanning quantum microscope used to probe local magnetic responses at the nanoscale. (b) Phase diagram of a 5.1 nm thick NbSe₂ flake as a function of temperature and magnetic field, identifying three distinct phases: vortex glass, vortex liquid, and a metallic state. (c) Magnetic field map of the vortex glass phase, showing pronounced field contrast and highlighting the sample boundary. (d) High-resolution scan resolving a single vortex in the NbSe₂ flake.

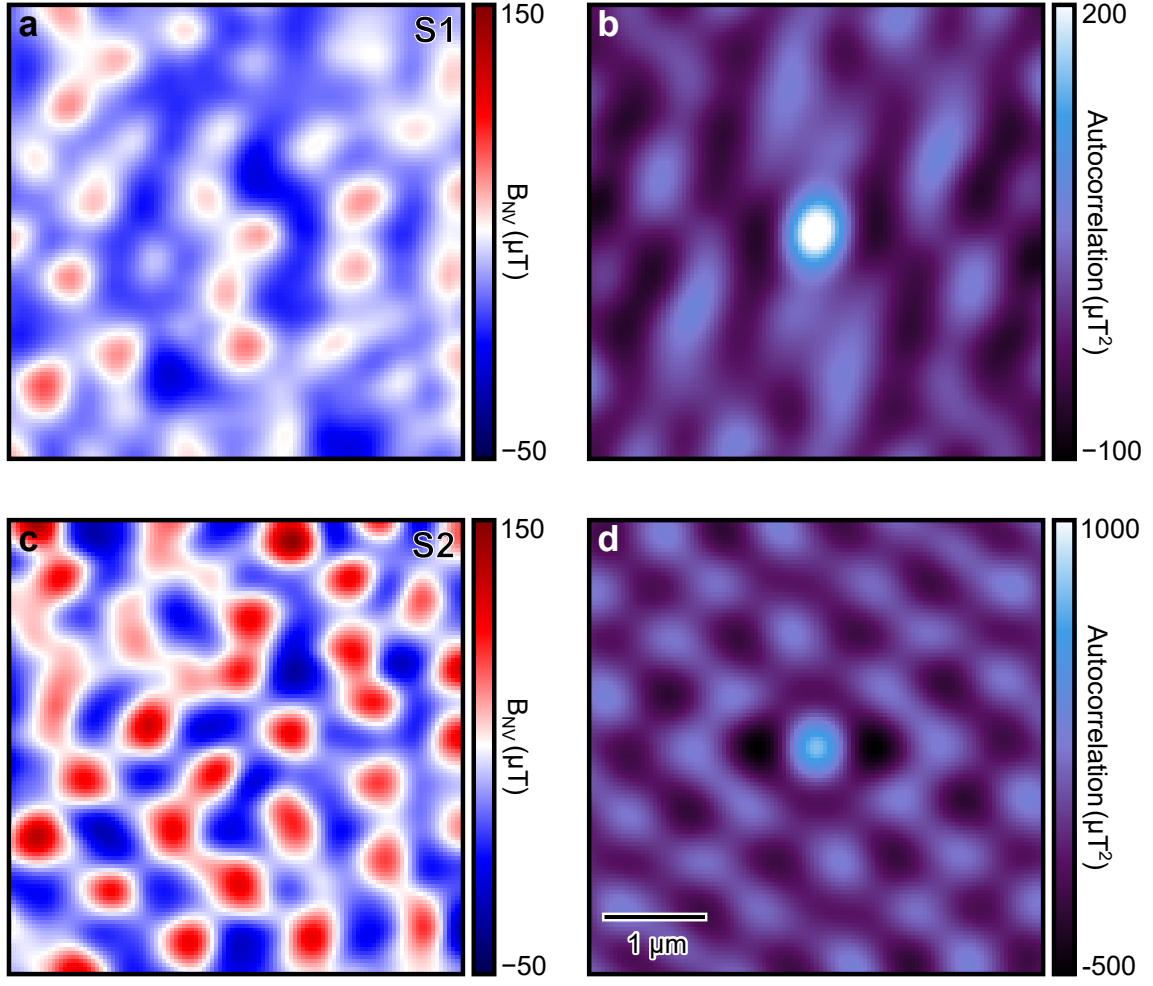


Fig. 2 Vortex arrangements in 2D NbSe₂ with varying thickness. (a, b) Magnetic field map and corresponding autocorrelation of a thin (5.1 nm) NbSe₂ sample S1 on an oxide substrate and encapsulated with hBN. The vortex configuration appears disordered, showing weak spatial correlations and broad, smeared autocorrelation peaks. (c, d) Magnetic field map and autocorrelation of a thicker (11.59 nm) NbSe₂ sample S2, fully encapsulated with hBN, revealing enhanced vortex hexagonal ordering.

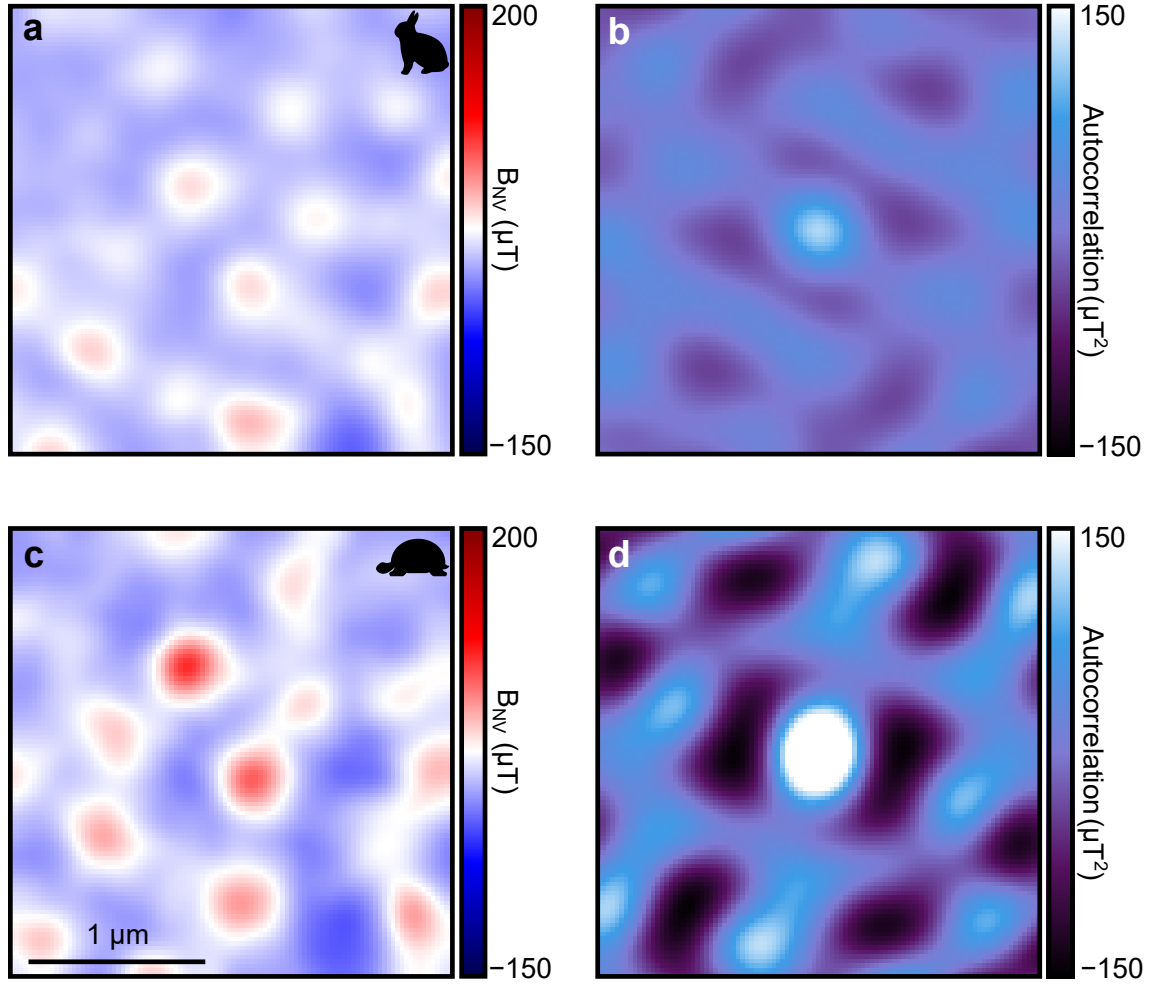


Fig. 3 Cooling rate-dependent vortex arrangements in 5.1 nm NbSe₂ sample S1. (a) SQM stray field map of a thin NbSe₂ flake after rapid cooling (from 6.3 K to 2 K within 1 minute), showing weak magnetic contrast. (b) Corresponding autocorrelation reveals a disordered vortex configuration with poor spatial correlation. (c) Magnetic field map after slow cooling (from 6.3 K to 2 K over several hours), showing enhanced vortex contrast. (d) Autocorrelation of (c) indicates more distinct local vortex ordering and stronger magnetic response.

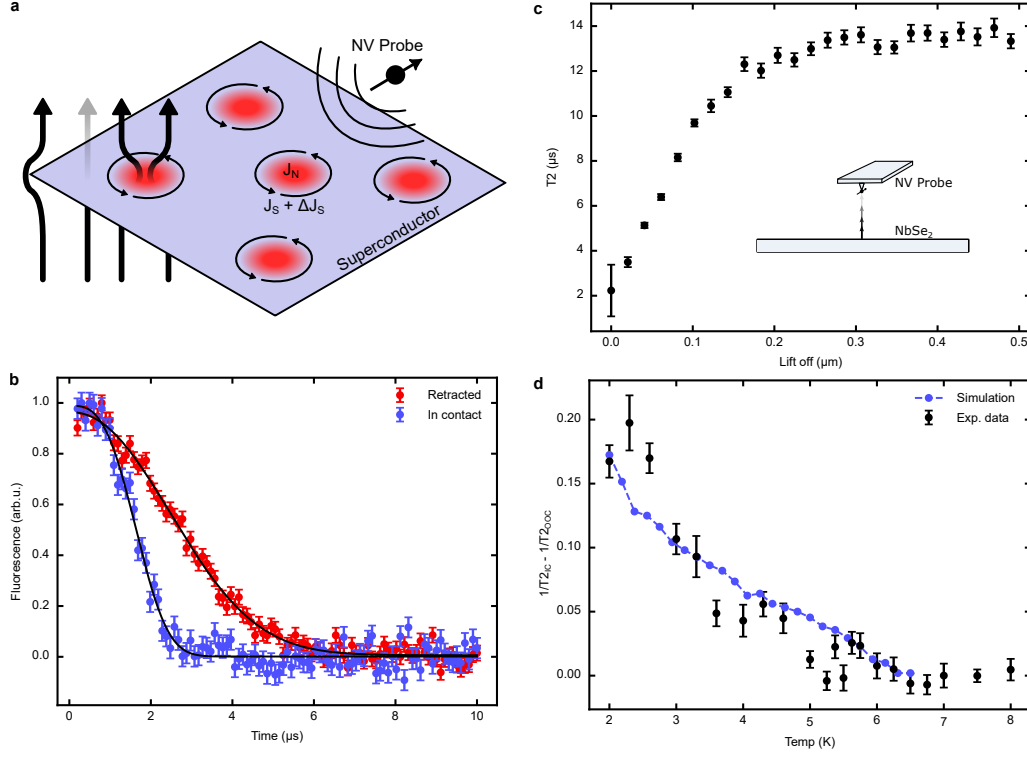


Fig. 4 Unexpected magnetic noise in 2D superconductors. (a) Schematic of a local NV probe detecting supercurrent-induced magnetic fluctuations in a 2D superconductor. Magnetic fields are only partially screened in the thin superconducting layer. (b) Spin Hahn echo T_2 measurements with the NV probe in contact with and retracted from the sample, revealing enhanced dephasing near the surface. (c) Extracted T_2 times as a function of lift-off distance. These data suggest that there is a critical length scale for magnetic fluctuations >100 nm. (d) Enhanced decoherence rate between in-contact and out-of-contact conditions ($1/T_{2IC} - 1/T_{2OOC}$), measured below the superconducting transition temperature (black dots). This rate reveals magnetic noise originating from the superconducting sample and exhibits an inverse temperature dependence, in good agreement with numerical simulations (blue dots).